



Deposited via The University of Leeds.

White Rose Research Online URL for this paper:

<https://eprints.whiterose.ac.uk/id/eprint/124500/>

Version: Accepted Version

---

**Article:**

García-Aguilar, J, Fernandez-Garcia, J, Rebrov, EV et al. (2017) Magnetic zeolites: novel nanoreactors through radiofrequency heating. *Chemical Communications*, 53 (30). pp. 4262-4265. ISSN: 1359-7345

<https://doi.org/10.1039/C7CC01138E>

---

© Royal Society of Chemistry 2017. This is an author produced version of a paper published in *Chemical Communications*. Uploaded in accordance with the publisher's self-archiving policy.

**Reuse**

Items deposited in White Rose Research Online are protected by copyright, with all rights reserved unless indicated otherwise. They may be downloaded and/or printed for private study, or other acts as permitted by national copyright laws. The publisher or other rights holders may allow further reproduction and re-use of the full text version. This is indicated by the licence information on the White Rose Research Online record for the item.

**Takedown**

If you consider content in White Rose Research Online to be in breach of UK law, please notify us by emailing [eprints@whiterose.ac.uk](mailto:eprints@whiterose.ac.uk) including the URL of the record and the reason for the withdrawal request.

DOI: 10.1002/((please add manuscript number))

**Article type: Communication**

## **Magnetic Zeolites: Novel Nanoreactors Through Radiofrequency Heating**

*Jaime García-Aguilar<sup>§</sup>, Javier Fernández-García<sup>§</sup>, Evgeny V. Rebrov, Martin Richard Lees, Pengzhao Gao, Diego Cazorla-Amorós, and Ángel Berenguer-Murcia\**

MSc. Jaime García-Aguilar <sup>a</sup>, Prof. Diego Cazorla-Amorós <sup>a</sup>, and Dr. Ángel Berenguer-Murcia <sup>a</sup>

<sup>a</sup> Inorganic Chemistry Department and Materials Science Institute, Alicante University, Ap. 99, E-03080 Alicante, Spain

Javier Fernández-García <sup>b</sup>, Prof. Evgeny V. Rebrov <sup>b, c</sup>, Dr. Martin Richard Lees <sup>b</sup>

<sup>b</sup> University of Warwick, Coventry, CV4 7AL, United Kingdom

<sup>c</sup> Department of Biotechnology and Chemistry, Tver State Technical University, Tver 170026, Russia

Pengzhao Gao <sup>d</sup>

<sup>d</sup> College of Materials Science and Engineering, Hunan University, Changsha, 410082, China

\* E-mail: [a.berenguer@ua.es](mailto:a.berenguer@ua.es)

<sup>§</sup> These authors contributed equally to the manuscript

**Keywords:** zeolites, magnetism, nickel ferrites, radiofrequency heating, catalysis

Beyond the traditional interest of colloidal particles with controlled structure, functionality, and/or morphology for the development of packed columns for separation or as catalyst carriers,<sup>[1]</sup> the synthesis of magnetic nanoparticles has recently aroused great attention as novel hybrid materials due to the fact that they combine the aforementioned characteristics with their responsiveness under a high frequency magnetic field which brings forth other very interesting and exciting features such as the ease of separation or the possibility of heating said particles using a radiofrequency coil.<sup>[2-3]</sup> In this respect, while the preparation of different magnetic nanoparticles is very well-established, with iron and its oxides being the most prominent example, the development of functionalization treatments of high quality to yield materials with superior properties still remains a largely unexplored field, even if significant progress has been reported in the use of different organic and inorganic passivation or functionalization agents.<sup>[4]</sup>

With their exceptional properties in the fields of adsorption and catalysis<sup>[5]</sup> deriving from a crystalline structure with molecular sieving properties combined with an outstanding framework acidity, zeolites are outstanding candidates for the development of advanced composites<sup>[6]</sup> combined with different species, with magnetic nanoparticles being one of the possibilities with very promising prospects. The recent work of Zhao *et al.*<sup>[1]</sup> and Al-Deyab *et al.*<sup>[7]</sup> have laid the groundwork for two different approaches to the preparation of zeolite-coated magnetic nanoparticles. The first involves coating the as-synthesized magnetic nanoparticles, while the second is achieved via the impregnation of zeolite particles with iron salts in order to give rise to magnetic nanoparticles after heat treatment of the resulting composites. Following up on this work, several authors have reported the use of these magnetic zeolites in the removal of different contaminants. For example, Yu *et al.* used magnetic particles impregnated into zeolite A to remove ammonium<sup>[8]</sup> from water, whereas Frost *et al.*<sup>[9]</sup> added magnetite particles to a zeolite A precursor solution in order to give rise to magnetic zeolites which could remove heavy metal ions from aqueous solutions. These examples, however, make use of the zeolite as a layer which does not play an active role, merely being an adsorbent for different species, with the added benefit of handling and separation efficiency. The only case which may be found in the literature in which the oxide layer surrounding a magnetic nanoparticle is effectively used as a reaction system is in very recent work from Cheng *et al.*<sup>[10]</sup> in which they synthesize TS-1 layers around different magnetic iron oxide species, and these composites are tested in the photocatalytic degradation of organic contaminants. It should be noted that, even in this example, the reactions are carried out at room temperature, without fully benefitting from any possible synergistic effects between the particle shell and core beyond the well-established ease of separation arising from their magnetic response. Previous reports on the synthesis and application of core@shell particles have endeavored to combine the properties of both parts of the material so that they may act in a combined and effective manner. Okada *et al.*<sup>[11]</sup> presented a new

type of core-shell structured catalyst to enable the one-pot oxidation of sulfide to sulfoxide with high efficiency and selectivity, in which a uniform SiO<sub>2</sub> core supporting Pd nanoparticles was covered with a Ti-containing mesoporous silica shell. Mori *et al.* <sup>[12]</sup> achieved the encapsulation of iron oxide nanoparticles within a silica matrix for the liquid-phase selective oxidation reactions of organic compounds using H<sub>2</sub>O<sub>2</sub> as oxidant. Nishiyama *et al.* <sup>[13]</sup> synthesized zeolite-encapsulated Pt/TiO<sub>2</sub> catalysts and applied these materials in the hydrogenation of different C<sub>6</sub> hydrocarbon mixtures, with the zeolite layer acting as a permselective barrier and the particle core playing an active role hydrogenating the permeating reagents. In this respect, it would be interesting if the core of a magnetic zeolite could contribute to the performance of the prepared material in a manner different (yet complementary) to what has been reported to date.

In this work we aim to prepare zeolite shells encapsulating magnetic nanoparticles by submitting a suspension of TiO<sub>2</sub>-coated nickel ferrite nanoparticles to hydrothermal treatment (static or dynamic) in an aqueous ZSM-5 precursor solution. The resulting composites show a ferrite core with a well-defined shell of zeolite ZSM-5 with a mean particle size ranging between 0.5 and 2 microns, and show a coercive field of  $\approx 0.0085$  T and a permanent magnetization of  $\approx 0.2$  A·m<sup>2</sup>/kg (which would correspond to 0.34 wt% of magnetic material in the composite materials, see Figure S1), and exhibit good dispersability in water. The resulting solids are then applied in the isomerisation reaction of citronellal to isopulegol with very promising results. This paper thus constitutes a landmark in the combination of radiofrequency heating in ferrite@zeolite particles for the development of nanoreactors with an unparalleled level of reaction control.

In a typical synthesis, the nickel ferrite nanoparticles were synthesized following a synthetic protocol adapted from the literature <sup>[14]</sup>. A portion of these magnetic nanoparticles with a magnetic domain size between 40 and 50 nm (calculated from their coercivity) was dispersed by means of an ultrasound probe using an aqueous solution of tetrapropylammonium

hydroxide (TPA-OH) which in this case not only acts as templating agent for the zeolite which is grown around the magnetic nanoparticle (ZSM-5 in this case), but also as a surfactant which adsorbs on the nanoparticles surface, facilitating their dispersion (the ferrite particles sedimented in a few seconds after sonication in the absence of TPA-OH). After sonication, the obtained dispersion was used in the hydrothermal synthesis of a zeolite in order to encapsulate each magnetic nanoparticle in a zeolite shell as described in the Experimental section. Two different growth regimes were employed: one in which the autoclaves were left standing inside the oven (static synthesis) and another in which the autoclaves were rotated inside the oven to ensure homogeneous crystallization of the zeolite (dynamic synthesis). In both cases, however, while no uncoated magnetic particles were observed (Figure S2 shows two TEM images in which the morphology and size of the uncoated ferrite particles can be clearly observed), there was a significant fraction of zeolite crystals which were formed in solution rather than encapsulating the nickel ferrite particles. This fact is revealed in **Figure 1**, which shows the SEM and TEM images of a sample obtained in the dynamic synthesis, where particles with distinct surface morphologies are observed; the particles with a characteristic coffin shape and smooth surface are ZSM-5 crystals which had grown in solution whereas the particles in which the planes grown along the *a* and *c* directions are significantly different from typical MFI zeolites (what we may call a “rough grain” surface) were the magnetic ferrite nanoparticles encapsulated in very small zeolite crystals.

It must be noted that the same micrographs taken from the samples obtained under static conditions showed a similar type of nanoparticles, although the fraction of particles with a rough grain surface was smaller than that obtained under dynamic conditions (Figure S3), confirming that conditions favoring homogeneous crystallization were more conducive towards the successful coating of ferrite nanoparticles. X-Ray diffraction analysis (results shown in Figure S4) confirmed the presence of both MFI and ferrite phases in all samples.

Nitrogen physisorption analyses (Table S1) revealed that samples prepared by both methods had similar porosities, with the samples obtained under dynamic conditions showing a slightly higher value (350 and 310 m<sup>2</sup>/g for the dynamic and static sample, respectively) which may be attributed to the fact that the apparent surface area values are rather high due to increased adsorption on the surface roughness. The pore volume values obtained for both samples were practically identical (0.15 and 0.14 cm<sup>3</sup>/g for the two samples), which is slightly lower than previously reported values for this type of zeolites<sup>[15]</sup>. In this respect, this difference may be accounted for by the presence of the non-porous nickel ferrite in the composite.

It must be noted that the TiO<sub>2</sub> shell deposited around the nickel ferrite nanoparticles was critical for the successful preparation of the core@shell structure reported in this study. When bare nickel ferrite nanoparticles were added to the autoclaves and submitted to hydrothermal treatment the filtered solid particles did not contain any ferrite particles (evidenced both by their colour and the corresponding TEM images). Thus, the TiO<sub>2</sub> shell plays a key role in the successful preparation of core@shell structures, acting as a linker under the employed conditions, as we have reported for similar systems<sup>[16]</sup>

Benefitting from the fact that the core of the composite nanoparticles is sensitive to a magnetic field (the magnetic heating generation rate was determined for both sets of samples presenting a value of  $\approx 0.2$  W/g), the reactor configuration was chosen so as to achieve efficient isothermal heating (see *Experimental*)<sup>[17]</sup>. As shown in **Figure 2**, the packed bed configuration not only allows one to reach the desired reaction temperature within seconds of applying the RF field, but also allows the reaction temperature to be controlled within a very narrow range (around 2 K). Additionally, this configuration also avoids the formation of non-uniform temperature distributions and hot spots<sup>[18]</sup> and overcomes the drawbacks in the scale-up of microreactors<sup>[19]</sup>. Such a configuration has an inherently large surface area-to-volume ratio, offering high heat and mass transfer rates, which is beneficial for attaining high conversion rates and enables optimum control of residence time and temperature distribution.

Moreover, the results for this configuration with nickel ferrite were satisfactory in previous work <sup>[17, 20]</sup> but now the magnetic contribution from the magnetic zeolite to the RF heating makes the profile more stable. The results obtained show that citronellal isomerisation has been successfully achieved with radiofrequency heating. Radiofrequency heating with magnetic materials has previously been used for other reactions <sup>[17, 20]</sup> and has been shown to be a suitable way to produce heating, even on an industrial scale <sup>[19]</sup>. This new magnetic material widens the possibilities for using radiofrequency heating as a more efficient, green alternative to conventional heating that can be applied on an industrial scale.

Most importantly, heating is restricted to the core-shell particles (specifically to their core), and thus this type of reactor is both novel in its conception and of almost unrivalled efficiency. Considering the data obtained for the isomerisation of citronellal presented in **Figure 3** (main panel), a linear dependence of reaction rate with the reactant concentration suggests a first order dependence with respect to citronellal. Moreover the light-off curves overlapped for the different initial concentrations, also indicating a linear dependence. As the temperature increases from 323 to 353 K, the citronellal conversion increases from 6 to 22 % (see the light-off curves for this reaction in Figure S5). The isomerisation of citronellal was performed over the magnetic zeolite (specifically ZSM-5) which provides a high isomerisation rate due to its high Brønsted acidity <sup>[21]</sup>. The apparent activation energy of 44.9 kJ/mol was obtained from the temperature dependence of the reaction rates. A comparable value of 55 kJ/mol was reported by Yongzhong et al. <sup>[22]</sup> over a Zr/Beta zeolite catalyst. No further studies were performed above the 353 K limit as a rapid catalyst deactivation was observed above 80 °C in line with the data reported by Makiarvela et al. <sup>[23]</sup>.

The catalyst is stable as no deactivation is observed for a period of 120 minutes. The catalyst seems to be stable reaching a constant conversion of 22%. Mass of the catalyst was measured before and after the reaction showing a difference around 0.5 % which indicates good mechanical stability of the magnetic catalyst. Moreover, this new magnetic zeolite allows the

simple separation of the catalyst with an external magnet <sup>[24]</sup>, which as already mentioned adds up to the added value of the active phase in terms of handling and reuse. This kind of reaction has become one of the most active research areas in pharmaceutical and fine chemical industries <sup>[25-28]</sup>.

For comparison purposes, the same microreactor experiments were performed with a physical mixture of ferrite and zeolite. The first attempts to prepare physical mixtures with compositions as similar as possible to our core@shell composite (2/98 % w/w) resulted in highly heterogeneous mixtures which performed very poorly in the isomerization of citronellal. Thus, we increased the amount of nickel ferrite until a homogeneous mixture was obtained, which was 50/50 % w/w. In Table S2, it can be seen that the normalized reaction rate for the physical mixture is quite similar to the one obtained for the magnetic composite. Therefore this means that the properties of the zeolite do not change considering the intrinsic ferrite. The surface area and pore volume for this zeolite in the physical mixture were analyzed before and after the reaction, with negligible changes in both the surface area and the pore volume of the mechanical mixture, with values very similar to those mentioned above. All these measurements involve that the physical mixture can be assumed as similar to the magnetic composite and its properties are not affected after the reaction, so the catalyst is stable.

In summary,  $\text{TiO}_2\text{-NiFe}_2\text{O}_4\text{@zeolite}$  (ZSM-5) particles have been synthesized by a simple two-step process in which  $\text{TiO}_2$ -coated nickel ferrite particles are coated with a layer of ZSM-5 zeolite crystals after dispersion in the presence of a surfactant (which is the zeolite structure directing agent). Performing the hydrothermal synthesis of the zeolite layer using dynamic conditions allows for a larger fraction of coated ferrite particles over the static synthesis, which ultimately results in a higher yield towards the desired product. The resulting core@shell structures have been incorporated in a structured reactor configuration in which citronellal is isomerized to isopulegol with exceptional control of the conditions inside the

reactor, allowing for the development of reactors and reaction systems with outstanding performance and stability, surpassing by a 25-fold factor the behaviour of a similar physical ferrite/zeolite mixture.

### **Experimental Section**

*Synthesis of magnetic nanoparticles:* Nanosized NiFe<sub>2</sub>O<sub>4</sub> nanoparticles were prepared by the citrate precursor method. Iron (III) nitrate nonahydrate, nickel nitrate hexahydrate, citric acid, ethanol, and ammonia solution (Sigma-Aldrich, ACS grade) were used for the preparation of the starting sol. The metal nitrates were dissolved in ethanol in the required molar ratios. Then a solution of citric acid in ethanol was added into the nitrate solution. The resulting solution was stirred for 4 h. The resulting sol was dried at 353 K to get a dry gel which was milled and calcined in air at 1073 K for 1 h (heating rate of 10 K/min) to produce the corresponding nickel ferrite nanoparticles.

The obtained nanoparticles were redispersed in an ethanol-water (80:20 v/v) solution containing 1 mol/L ammonia and 3 mmol/L cetyltrimethylammonium bromide (Sigma-Aldrich) to prepare a solution with a final concentration of 0.135 mg nanoparticles/mL (Solution A). The titania sol was prepared by dissolution of a tetrabutyltitanate-diethanolamine mixture (80:20 v/v, Sigma-Aldrich) in ethanol. The hydrolysis of the sol was performed by dropwise addition of an ethanol-water solution (90:10 v/v) to the titania sol. The resulting mixture was stirred for 24 h and then left under static conditions for another 24 h. Afterwards it was added dropwise to solution A under vigorous stirring. The obtained solids were centrifuged, washed by ethanol twice and then dried in an oven and calcined under air flow at 673K for 1 h with a heating rate of 1 K/min. According to the elemental analysis data, the titania loading in the TiO<sub>2</sub>-NiFe<sub>2</sub>O<sub>4</sub> nanoparticles was 6 wt%.

*Synthesis of zeolite-encapsulated magnetic nanoparticles:* The as-synthesized nickel ferrite nanoparticles were coated with a layer of ZSM-5 zeolite with a procedure which was adapted from the literature.<sup>[6,29]</sup> The powdered solid was first dispersed in a 1M aqueous solution of tetrapropylammonium hydroxide (TPA-OH) by sonication for 2.5 minutes with an ultrasound probe (Bandelin Sonoplus GM2200, 200 W) at 40% of output power. In order to use as homogeneous a suspension as possible, the sonicated samples were left standing for 1 day and only the supernatant was used for the synthesis of the core@shell samples. The relative amounts of magnetic nanoparticles and TPA-OH solution were 4575 and 50 milligrams, respectively. Aluminium (III) isopropoxide (gentle heating was applied to facilitate dissolution of the aluminium salt), sodium hydroxide, distilled water and tetraethylorthosilicate (TEOS) were added to the magnetic nanoparticle suspension to yield a clear precursor solution (with a brownish colour arising from the presence of the ferrite nanoparticles). Sonication was applied for 2.5 minutes at 40% output power after the addition of the aluminium precursor and again after the silica precursor addition. The resulting zeolite precursor solution had the composition: 1 Al<sub>2</sub>O<sub>3</sub>:50 SiO<sub>2</sub>: 990 H<sub>2</sub>O:18 TPA-OH: 0.32 NaOH. This solution was then transferred to a Teflon-lined stainless steel autoclave and hydrothermal synthesis was performed in a convection oven at 438 K for 5 days. The hydrothermal treatment was performed both under static and dynamic conditions. In the former, the autoclaves were left standing in the oven, whereas in the latter the autoclaves were rotated inside the oven at a speed of 20 revolutions/minute in order to ensure a homogeneous crystallization of the zeolite around the ferrite nanoparticles. The as-synthesized samples were filtered, washed with abundant distilled water, and dried in an oven at 333 K overnight. The samples were calcined at 723 K for 12 hours.

*Characterization:* The samples prepared in this study were characterized by transmission electron microscopy (TEM) using a JEOL JEM-120 microscope. The composition of the magnetic nanoparticles was measured by EDS coupled to the TEM equipment (OXFORD

instruments model INCA energy TEM100). The external morphology of the samples was also analyzed by field emission scanning electron microscopy (FE-SEM, Merlin VP Zeiss) in order to assess the quality and extent of the zeolite coating around the ferrite nanoparticles. The N<sub>2</sub> adsorption isotherms were obtained at 77 K using an ASAP2020 apparatus (Micromeritics). The magnetization curves were recorded at 293 K with a vibrating sample magnetometer (Oxford Instruments). The X-ray diffraction patterns were obtained in the 10-80° 2θ range at a rate of 0.02° min<sup>-1</sup> with a diffractometer (Pan Analytical Empyrean). The specific absorption rate under RF heating was determined using a 1 kW induction heating system operated at 300 kHz (Ambrell EasyHeat®).

The catalytic activity in the isomerization of citronellal was measured in a quartz reactor (i.d. 9.5 mm). The reactor was placed inside a 6-turn induction coil connected to the 300 kHz induction heating system. The gas and liquid flows were fed in co-current mode from the top. A solution of citronellal (40-80 mM) in 1,4-dioxane was fed to the reactor with an HPLC pump (Shimadzu LC-20AT, liquid flow rate 0.1 mL/min). A He flow of 3.0 ml/min (STP) was fed with a mass flow controller (Brooks). The gas flow provides a more uniform distribution of the liquid and prevents bed densification which improves hydrodynamics in the reactor as demonstrated in our previous work <sup>[17, 20]</sup>.

Prior to the assembly of the structured reactor, the magnetic core@shell particles were purified applying a high-power magnet to a suspension of the powdered solid in water. This was done in order to ensure that the catalyst bed was composed of magnetic ferrite@zeolite particles. A bed of glass beads mixed with magnetic particles of nickel ferrite was placed at the initial section of the catalyst bed to provide uniform flow distribution and preheat the reaction mixture to the desired temperature. In order to maintain an isothermal temperature profile inside the reactor, the catalyst bed was placed between two beds of nickel ferrite particles as this configuration was found to be efficient in maintaining isothermal conditions in our previous work <sup>[17]</sup>. The structured bed (nickel ferrite/catalyst/nickel ferrite) was kept in

the middle part of the reactor with two porous PEEK plates. The movable optical fiber temperature sensor (FISO FPI HR) was placed inside a thin glass well along the center line of the catalyst bed to monitor the bed temperature. The temperature of the reactor was controlled within 0.5 K with a LabVIEW software. The reaction products were analysed on a gas chromatograph (Shimadzu GC-2010) equipped with a CP-Sil column and an FID detector.

### Supporting Information

Supporting Information is available from the Wiley Online Library or from the author.

### Acknowledgements

We thank the MINECO, GV, and FEDER (Projects CTQ2015-66080-R and PROMETEOII/2014/010) for financial support. J.G.A. thanks the Spanish Ministry of Economy and Competitiveness (MINECO) for his fellowship (BES-2013-063678). Moreover, the financial support provided by the European Research Council (ERC), project 279867, and Russian Science Foundation (project 15-13-20015) is gratefully acknowledged.

Received: ((will be filled in by the editorial staff))

Revised: ((will be filled in by the editorial staff))

Published online: ((will be filled in by the editorial staff))

[1] Y. Deng, C. Deng, D. Qi, C. Liu, J. Liu, X. Zhang, D. Zhao, *Adv. Mater.* **2009**, 21, 1377.

[2] P. Gao, E.V. Rebrov, M.W.G.M. Verhoeven, J.C. Schouten, R. Kleismit, G. Kozłowski, J. Cetnar, Z. Turgut, G. Subramanyam, *J. Appl. Phys.* **2010**, 107, 044317-1.

[3] A. Zadrazil, V. Tokarova, F. Stepanek, *Soft Matter* **2012**, 8, 6, 1811.

- [4] W. Wu, Q. He, C. Jiang, *Nanoscale Res. Lett.* **2008**, 3, 397.
- [5] E.G. Derouane, *J. Molec. Catal. A* **1998**, 134, 29.
- [6] A. Berenguer-Murcia J. García-Martínez, D. Cazorla-Amorós, A. Linares-Solano, A.B. Fuertes, *Micropor. Mesopor. Mater.* **2003**, 59, 147.
- [7] T.A. Salah El-Din, A.A. Elzatahry, D.M. Aldhayan, A.M. Al-Enizi, S.S. Al-Deyab, *Int. J. Electrochem. Sci.* **2011**, 6, 6177.
- [8] M. Liu, B.-D. Xi, L.-A. Hou, S. Yu, *J. Mater. Chem. A*, **2013**, 1, 12617.
- [9] H. Liu, S. Peng, L. Shu, T. Chen, T. Bao, R.L.Frost, *Chemosphere* **2013**, 91, 1539.
- [10] Q. Lv, G. Li, H. Lu, W. Cai, H. Huang, C. Cheng, *Micropor. Mesopor. Mater.* **2015**, 203, 202.
- [11] S. Okada, K. Mori, T. Kamegawa, M. Che, H. Yamashita, *Chem. Eur. J.* **2011**, 17, 9047.
- [12] K. Mori, Y. Kondo, S. Morimoto, H. Yamashita, *J. Phys. Chem. C* **2008**, 112, 397.
- [13] N. Nishiyama, K. Ichioka, M. Miyamoto, Y. Egashira, K. Ueyama, L. Gora, W. Zhu, F. Kapteijn, J.A. Moulijn, *Micropor. Mesopor. Mater.* **2005**, 83, 1-3, 244.
- [14] P. Gao, X. Hua, V. Degirmenci, D. Rooney, M. Khraisheh, R. Pollard, R.M. Bowman, E.V. Rebrov, *J. Magn. Magn. Mater.* **2013**, 348, 44.
- [15] S. Sartipi, K. Parashar, M.J. Valero-Romero, V.P. Santos, B. van der Linden, M. Makkee, F. Kapteijn, J. Cascon, *J. Catal.* **2013**, 305, 179.
- [16] J. García-Aguilar, I. Miguel-García, Á. Berenguer-Murcia, D. Cazorla-Amorós, *ACS Appl. Mater. Interfaces* **2014**, 6, 22506.
- [17] S. Chatterjee, V. Degirmenci, F. Aiouache, E.V. Rebrov, *Chem. Eng. J.* **2014**, 243, 225.
- [18] J.G. Boelhouwer, H.W. Piepers, A.A.H. Drinkenburg, *Chem. Eng. Sci.* **2001**, 56, 1181.
- [19] J. Fernandez, S. Chatterjee, V. Degirmenci, E.V. Rebrov, *Green Process. Synth.* **2015**, 4, 343.

- [20] S. Chatterjee, V. Degirmenci, E.V. Rebrov, *Chem. Eng. J.* **2015**, 281, 884.
- [21] P. Maki-Arvela, N. Kumar, V. Nieminen, R. Sjoholm, T. Salmi, D.Y. Murzin, *J. Catal.* **2004**, 225, 155.
- [22] Z. Yongzhong, N. Yuntong, S. Jaenicke, G.K. Chuah, *J. Catal.* **2005**, 229, 445.
- [23] J.G. Boelhouwer, H.W. Piepers, A.A.H. Drinkenburg, *Chem. Eng. Sci.* **2001**, 56, 1181.
- [24] T.K. Houlding, E.V. Rebrov, *Green Process. Synth.* **2012**, 1, 19.
- [25] M.J. Climent, A. Corma, S. Iborra, M.J. Sabater, *ACS. Catal.* **2014**, 4, 870.
- [26] D.E. Fogg, E.N. dos Santos, *Coordin. Chem. Rev.* **2004**, 248, 2365.
- [27] X. Zeng, *Chem. Rev.* **2013**, 113, 6864.
- [28] D.M. Roberge, L. Ducry, N. Bieler, P. Cretton, B. Zimmermann, *Chem. Eng. Technol.* **2005**, 28, 318.
- [29] B.J. Schoeman, J. Sterte, J.-E. Otterstedt, *Zeolites* 1994, **14**, 110.

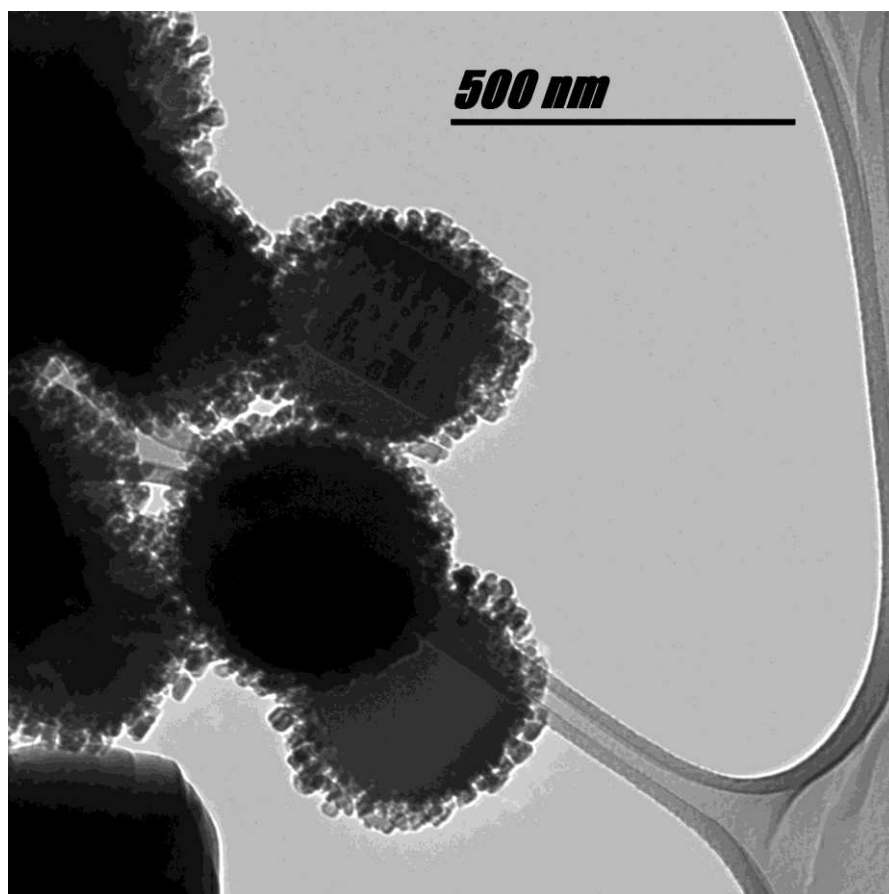
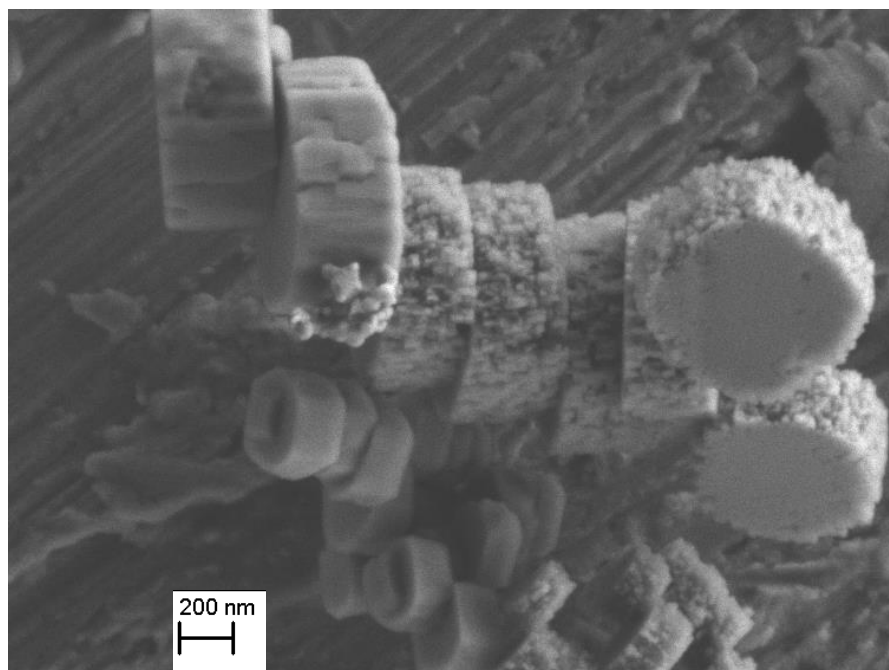


**Figure 1.** FE-SEM (top) and TEM (bottom) micrographs of the zeolite-encapsulated magnetic nanoparticles obtained under dynamic conditions.

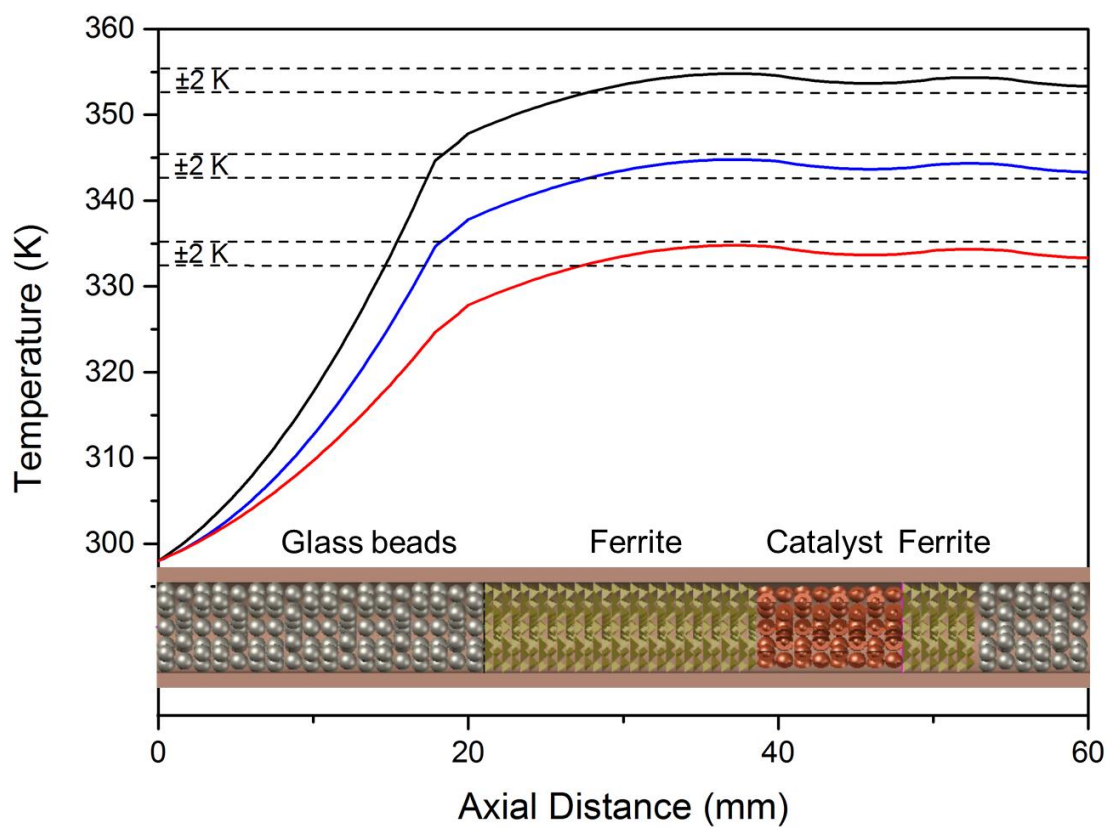


**Figure 2.** Temperature profiles in the reactor at three set-points of 333, 343 and 353 K. Catalyst weight: 82.2 mg. Liquid flow rate: 0.1 ml/min. Gas flow rate: 3.0 ml/min (STP).

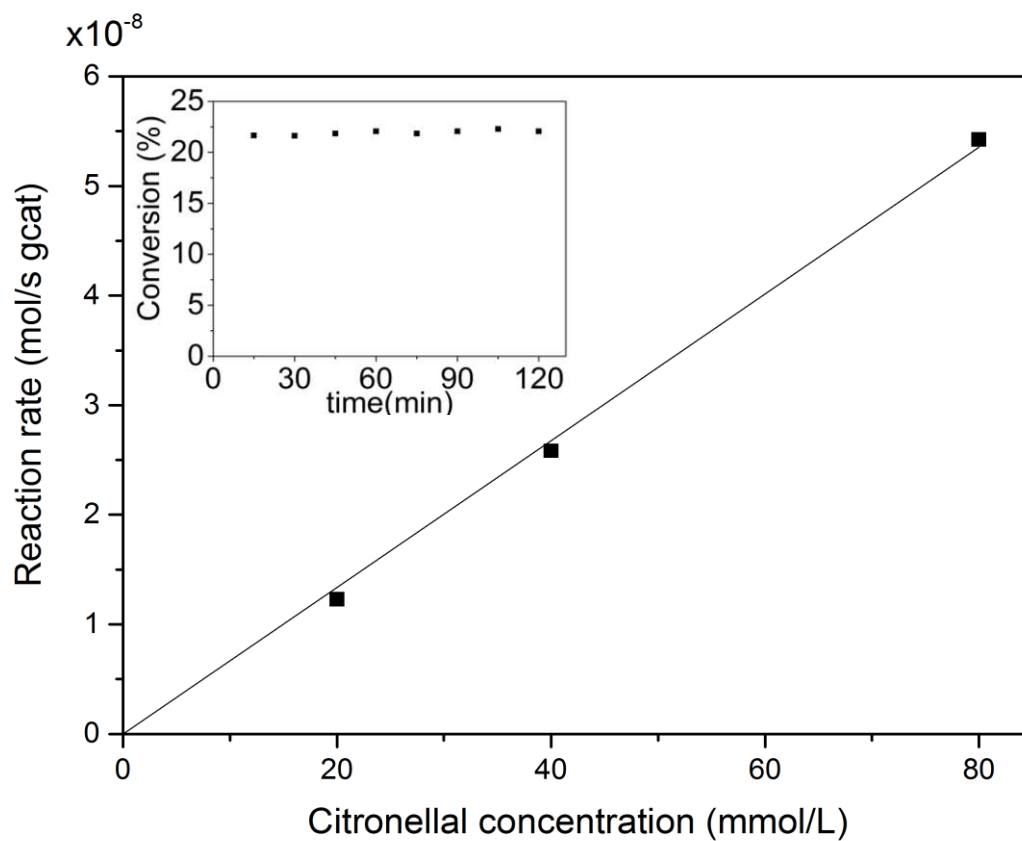


**Figure 3.** Reaction rate as a function of citronellal initial concentration. Temperature 353 K. Catalyst weight: 82.2 mg. Liquid flow rate: 0.1 ml/min. Gas flow rate: 3.0 ml/min (STP). Insert: Conversion as a function of time on stream.

**A new concept of chemical reactor is presented through the synergistic interaction of RF heating in core@shell particles.** Magnetic nickel ferrite nanoparticle encapsulated in a zeolite shell are submitted to a RF field in a packed bed, giving rise to a reactor in which the isomerization of citronellal can be carried out with unparalleled levels of efficiency and accuracy.

**Zeolites, magnetism, nickel ferrites, radiofrequency heating, catalysis**

*Jaime García-Aguilar, Javier Fernández-García, Evgeny V. Rebrov, Martin Richard Lees, Pengzhao Gao, Diego Cazorla-Amorós, and Ángel Berenguer-Murcia\**

**Magnetic Zeolites: Novel Nanoreactors Through Radiofrequency Heating**

ToC figure ((Please choose one size: 55 mm broad × 50 mm high **or** 110 mm broad × 20 mm high. Please do not use any other dimensions))

